REVIEWS

Journal of Semiconductors
(2024) 45, 011501
doi: 10.1088/1674-4926/45/1/011501

GaN based ultraviolet laser diodes

Jing Yang[1], Degang Zhao[1, 2, †], Zongshun Liu[1], Yujie Huang[1], Baibin Wang[1], Xiaowei Wang[1], Yuheng Zhang[1], Zhenzhuo Zhang[1], Feng Liang[1], Lihong Duan[1], Hai Wang[1], and Yongsheng Shi[1]

[1]State Key Laboratory on Integrated Optoelectronics, Institute of Semiconductors, Chinese Academy of Sciences, Beijing 100083, China
[2]School of Electronic, Electrical and Communication Engineering, University of Chinese Academy of Sciences, Beijing 100049, China

Abstract: In the past few years, many groups have focused on the research and development of GaN-based ultraviolet laser diodes (UV LDs). Great progresses have been achieved even though many challenges exist. In this article, we analyze the challenges of developing GaN-based ultraviolet laser diodes, and the approaches to improve the performance of ultraviolet laser diode are reviewed. With these techniques, room temperature (RT) pulsed oscillation of AlGaN UVA (ultraviolet A) LD has been realized, with a lasing wavelength of 357.9 nm. Combining with the suppression of thermal effect, the high output power of 3.8 W UV LD with a lasing wavelength of 386.5 nm was also fabricated.

Citation: J Yang, D G Zhao, Z S Liu, Y J Huang, B B Wang, X W Wang, Y H Zhang, Z Z Zhang, F Liang, L H Duan, H Wang, and Y S Shi, GaN based ultraviolet laser diodes[J]. *J. Semicond.*, 2024, 45(1), 011501. https://doi.org/10.1088/1674-4926/45/1/011501

1. Introduction

GaN-based nitride alloys, including InN, GaN, AlN, and their ternary alloy, have direct transition energy band and a tunable wide bandgap from 0.7 to 6.2 eV by controlling the AlN or InN mole fraction. Since the 1990s, GaN-based materials and devices have experienced rapid development, and have been regarded as the most promising materials for ultraviolet (UV) and visible light-emitting devices. UV laser diodes (LDs) have the advantage of a number of applications, such as material processing, bio-chemical analysis, excitation light source for phosphors and high photolithographic resolution. Thus, many studies have examined the fabrication of GaN based UV LDs. So far, GaN based UV LDs have been reported by many groups[1–17]. In 1997, the first InGaN UV LD in the world was fabricated by Nakamura *et al.* in Nichia Corporation. The lasing wavelength was 395 nm under continuous-wave (CW) operation at room temperature (RT)[9]. In 2003, Masui *et al*. shortened the emission wavelength of UV LD to 365 nm, its threshold current and voltage under CW operation was 50 mA and 4.8 V[6]. At the same time, they achieved a shorter UV LD with lasing wavelength of 354.7 nm under pulse current injection at 25 °C, but the threshold current increased significantly to 14.8 kA/cm^2. Then, in 2008, Yoshida *et al*. in Hamamatsu Photonics K.K reduced the wavelength of UV LD to 342 and 336 nm by hetero-facet-controlled epitaxial lateral overgrowth (hetero-FACELO) method[10, 11], and they further achieved a 338 nm UV LD with output power over 1 W under pulsed operation[12]. This remained the highest power value of UV LDs until 2022. However, further reducing lasing wavelength and increasing output power faces many challenges because of the large lattice mismatch between high AlN mole fraction AlGaN cladding layer and the GaN substrate. To date, the highest CW optical output power of a 375–380 nm GaN-based commercially produced LD is approximately 400 mW, which was fabricated by Nichia Corporation. As to UVB (ultraviolet B) and UVC (ultraviolet C) LDs with electric-injection emission, AlN substrate or AlN template must be used to reducing the stress in AlGaN cladding layers with high AlN mole fraction. The high defect density of AlN and AlGaN material, and low hole concentration in p-type AlGaN cladding layer are the main limiting factors. In 2019, Amano's group and Asahi Kasei Corporation cooperated to achieve the 271.8 nm UVC LD successfully by using distributed polarization doping (DPD) approach to achieve hole conductivity and injection[7]. This was the first UVC electrically injected LD in the world. Recently, they further reported a UVC LD under room temperature CW operation with largely reduced threshold voltage[13]. In general, in terms of UV LD, Japanese technology takes lead in the international research community. In China, our group realized UVA LDs with a lasing wavelength of 381.9 nm in 2016[14]. The lasing wavelength was further reduced to 357.9 nm in 2022[15, 16] and the RT CW output power of UVA LD increased to 3.8 W with a lasing wavelength of 386.5 nm[17, 18]. Although UV LDs have been investigated for many years, their performance is much lower than those of GaN based violet, blue, and green LDs. In this paper, the challenges of UV LDs, especially for lasing wavelengths from 320 to 400 nm, will be analyzed and approaches to improve their performance will be reviewed.

2. Challenges

The challenges for UV LDs are tremendous and depend strongly on the emission wavelength. As previously reported, the threshold current density increases with the reduction of lasing wavelength, especially when the wavelength is less than 380 nm[19]. This indicates that the difficulty for fabricating UV LDs increases largely with decreasing wavelength. In addition, UV LDs with high CW output power have rarely been reported. The typical epitaxial layer structure of GaN-based UV LDs includes n-AlGaN cladding layer (CL), lower AlGaN waveguide layer (LWG), active region, upper AlGaN

Correspondence to: D G Zhao, dgzhao@red.semi.ac.cn
Received 12 JUNE 2023; Revised 25 AUGUST 2023.

waveguide layer (UWG), high AlN mole fraction AlGaN electron blocking layer (EBL), p-AlGaN CL, and p-GaN contact layer. To realize laser diodes in the UV region with shorter wavelength and higher output power, the following four major technological barriers need to be overcome:

ⅰ) A superior optical cavity that enables the confinement of as much light as possible therein with a low optical loss is highly required. To increase the optical confinement factor and decrease optical loss, lasers emitting at shorter wavelength require high AlN mole fraction of AlGaN or InAlGaN in active regions and confinement heterostructures. The optimized UV LD structure of AlN mole fraction of AlGaN CL and WG layers is higher than 20% and 10%, respectively. The tensile strain of the AlGaN layer increases with increasing AlN mole fraction when it grows on free standing GaN substrates with low defect density[20]. Special strain relief techniques are required to avoid the formation of cracks in the laser heterostructure.

ⅱ) A semiconductor material with high optical gain is required. As for AlGaN-based semiconductors, if high-quality crystals are fabricated, very high optical gains in the several thousand should be obtained[21]. However, it has so far been difficult to obtain high-quality AlGaN crystals. Many kinds of defects, such as vacancy defect and dislocation, exist in AlGaN material. Meanwhile, the localization effect for carriers reported in InGaN material[22, 23] is weak in GaN or AlGaN materials. This results in serious nor-radiative recombination in waveguide layers and active region. Therefore, low carrier injection efficiency and radiative recombination efficiency often exist in UV LDs.

ⅲ) Because of the intrinsic requirement of stimulated emission in semiconductor lasers, the high-current-density operation, which enables population inversion of carriers in the active region, should be realized. This would result in serious leakage of carriers and a low wall plug efficiency (WPE). Furthermore, the characteristic temperature of UV LDs is often lower than blue-violet GaN based LDs, and thus the performance of UV LDs will degrade much faster due to increased Joule heating. This results in a thermal rollover phenomenon or catastrophic optical mirror damage (COMD), which further limits the increase of CW output power of UV LDs.

ⅳ) The high energy of ultraviolet photons with reduction of the lasing wavelength can easily destroy the cavity surface coating, increasing optical absorption loss. The selection of cavity coating material is more challenging, and the requirement for cleanliness of the cavity coating and hermetic tightness of packaging process of ultraviolet lasers is much stricter.

3. Progress

3.1. Mismatch stress relief of the AlGaN template

For the wavelength span of UVA (315–400 nm), especially for LDs with the lasing wavelength less than 370 nm, the optimized AlN mole fraction of AlGaN cladding layer is higher than 20%[1–6, 15–17]. Huge stress between AlGaN cladding layer and GaN underlayer may generate cracking in AlGaN epilayers. One solution to this problem is to use of epitaxially laterally overgrown (ELOG) and patterned GaN template to release the stress and suppress the generation of

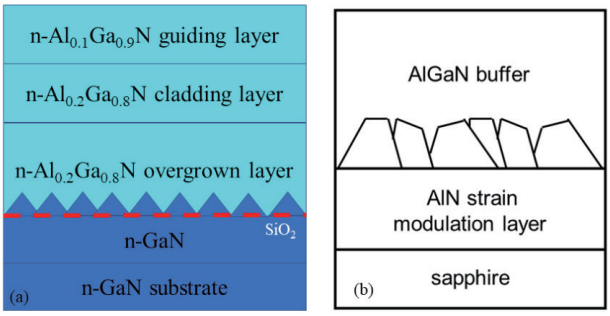

Fig. 1. (Color online) Schematic diagram of the sample structures for two different growth methods: ELOG method (a) and the method grown on AlN strain modulation layer (b).

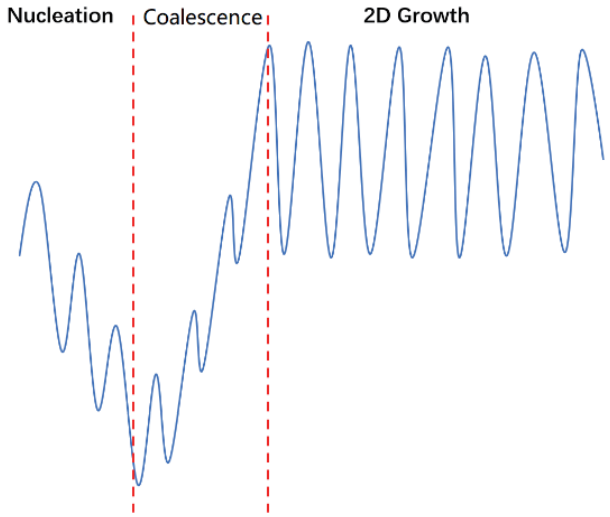

Fig. 2. (Color online) Schematic diagram of *in-situ* reflectance curve in initial stage of AlGaN growth[25].

cracking in AlGaN cladding layers. A schematic diagram of the sample structure is shown in Fig. 1(a). This is an effective method, and many groups have been realized GaN based UVA LDs based on the ELOG AlGaN templates[1–4, 24]. In 2007, Yoshida[24] succeeded in fabricating GaN/AlGaN UV LDs without crack generation on whole 2-in sapphire substrate by using hetero-FACELO method. The UV laser diodes lased in the peak wavelength range from 355.4 to 361.6 nm under a pulsed current operation at room temperature. In 2015, Aoki *et al.*[4] have demonstrated the pulsed operation of a 350-nm-band UV LD using patterned GaN substrate and ELOG technology, The lasing wavelength was 356.6 nm and the peak output power reached to 10 mW from the one side of uncoated facets.

In addition to ELOG templates, AlN modulation layer is another method to release stress and obtain a cracking free AlGaN layer with low stress and low dislocation density, which has been reported in our previous literature[25]. For this method, AlN strain modulation layer was first grown on sapphire substrate. Then, AlGaN layer with AlN mole fraction of about 20% was grown on the AlN strain modulation layer. A schematic diagram of our AlGaN template growth method is shown in Fig. 1(b). This can be described by three stages: (ⅰ) nucleation; (ⅱ) coalescence; and (ⅲ) two-dimensional (2D) growth, which have been marked by the dashed line in Fig. 2. For the nucleation stage, deposited AlGaN will form a large number of small grains first due to the mismatch strain

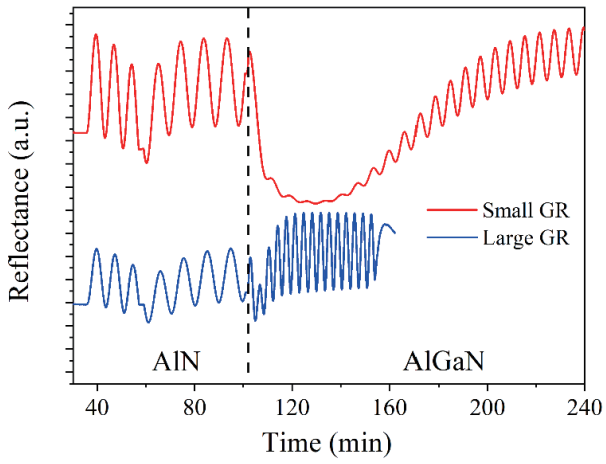

Fig. 3. (Color online) The *in-situ* reflectance curves of AlGaN samples with different growth rate (GR). The GR controlled by TMGa flow rate, it is 34.7 sccm for the sample with small GR, 69.4 sccm for the sample with large GR.

between AlGaN and AlN, in this case, the surface becomes rougher and rougher. The *in-situ* reflectance curve shows a drop at the nucleation stage. Then, at the coalescence stage, grains continue to grow and start to coalesce. The surface becomes smoother and the optical reflectance value rises. Finally, the reflectance stops to increase and 2D growth of the AlGaN begins. If the mismatch strain is released adequately at the nucleation and coalescence stages, then AlGaN will be relaxed in the beginning of 2D growth stage. Otherwise, the remaining stress will be released at the 2D growth stage by forming new dislocations, specifically, threading dislocations[26].

Based on this method, over 2 μm $Al_{0.18}Ga_{0.82}N$ template layer without crack was successfully grown on AlN/sapphire substrate. Its relaxation is about 90% and the AlN mole fraction is about 18%, the reflectance curves of two samples are shown in Fig. 3. The growth process is similar to the one shown in Fig. 2. However, the process from 3D to 2D is related to their growth conditions. It is shown that a much longer time is needed to achieve 3D to 2D growth when the GR of AlGaN layer reduces. The full width of half maximum (FWHM) values of X-ray diffraction (XRD) (002) and (102) reflection measured by rocking curves are decreased to (206, 315) for the sample with small GR. Compared with the values for the sample with large GR (153, 549), the FWHM values of the (102) reflection obviously decrease. This indicates that the density of edge dislocations reduces during the process from 3D to 2D.

3.2. Vacancy defect in AlGaN layers

Due to the large crystal mismatch and different atom mobility of Ga and Al atoms, the defect density in AlGaN material is as high as 10^8–10^{10} cm^{-3}. For UV LDs, AlGaN material must be used as waveguide layers and the active region. In this case, carrier injection efficiency and radiative recombination efficiency of MQWs may decrease due to the loss of carriers resulted from serious non-radiative recombination. Therefore, defect states in AlGaN layer and their suppression methods must be investigated. Previously, the influence of defects on performance of UV LDs have been investigated by many groups. Tsuzuki[27] fabricated a 358 nm UVA LD by using a GaN/AlGaN MQW active layer grown on a low dislocation density grooved-AlGaN template, which dislocation density was as low as 1×10^8 cm^{-2}. This UV LD exhibits a lower current density of 3.8 kA/cm^2 at 7 °C. In 2015, Crawford[28] applied overgrowth of AlGaN templates patterned with submicron mesas for achieving reduced-through dislocation density (TDD) templates of (2–3) $\times$ 10^8 cm^{-2} for AlGaN LDs. He successfully demonstrated pulsed-current operation of 353 nm wavelength LDs at room temperature.

Except for dislocations and impurities, point defects are also critical defects in AlGaN layers. We have used positron annihilation experiments to investigate point defects in AlGaN layers, and used responsivity of AlGaN detectors to judge the transport ability of carriers. Figs. 4(a) and 4(b) show the low-momentum parameter *S* and the high-momentum parameter *W* as functions of positron incident energy for the five AlGaN samples, where the AlN mole fraction of AlGaN is 0%, 2.6%, 3.77%, 5.44%, and 6.47% for samples T0, T1, T2, T3, and T4, respectively. Fig. 4(c) shows the relationship between *W* and *S* parameter of these five samples. It is found that as the AlN mole fraction increases, the *W* parameter value decreases and the *S* parameter value increases, the parameter *W* varies linearly with *S* for these five samples. This indicates that the only type of point defect in the AlGaN layer is mainly negatively charged[29] and its concentration increases with the increase of AlN mole fraction. Because this kind of point defect is a negative center, it is most likely to be a Ga vacancy defect because formation energy of Ga vacancy defect is slightly lower than that of Al vacancy defect[30, 31]. Fig. 4(d) shows the peak responsivity of AlGaN detectors and *S* parameter versus AlN mole fraction in i-AlGaN. Peak responsivity decreases with the increase of AlN mole fraction of AlGaN, indicating that the transport ability of carriers reduces in AlGaN with higher AlN mole fraction. This is consistent with the variation of vacancy density in AlGaN. It is necessary to control the concentration of vacancy defects for the AlGaN material to enhance the injection efficiency of carriers[32]. The investigation of influence of vacancy defects on the performance of UV LDs is underway.

We have also found that Ga vacancy defects act as acceptors in n-AlGaN layer, which passivate donors in Si dopped AlGaN. This increases the resistivity of the n-AlGaN layer[33]. Increasing the GR and reducing the growth temperature is helpful for suppressing the formation of Ga vacancy, and therefore a AlGaN film with resistivity as low as 0.005 Ω·cm can be obtained. The resistivity values as functions of AlN mole fraction of n-AlGaN layers reported by many groups are shown in Fig. 5, while our results are shown as red solid star symbols.

3.3. Observation of localization effect in GaN/AlGaN ultraviolet quantum well

Due to the fluctuation of the InN mole fraction in InGaN, In-rich clusters will form in the InGaN layer, which act as localization states for carriers and hinder carriers to defect to regions and recombine there. Therefore, the emission efficiency is very high, even though the dislocation density is as high as 10^8–10^{10} cm^{-3}[22, 23]. However, localization effects become weak when the InN mole fraction of InGaN decreases. The emission efficiency of UV quantum wells decreases rapidly and is more sensitive to dislocation density. This is harmful for UV LDs because the quantum well layers in

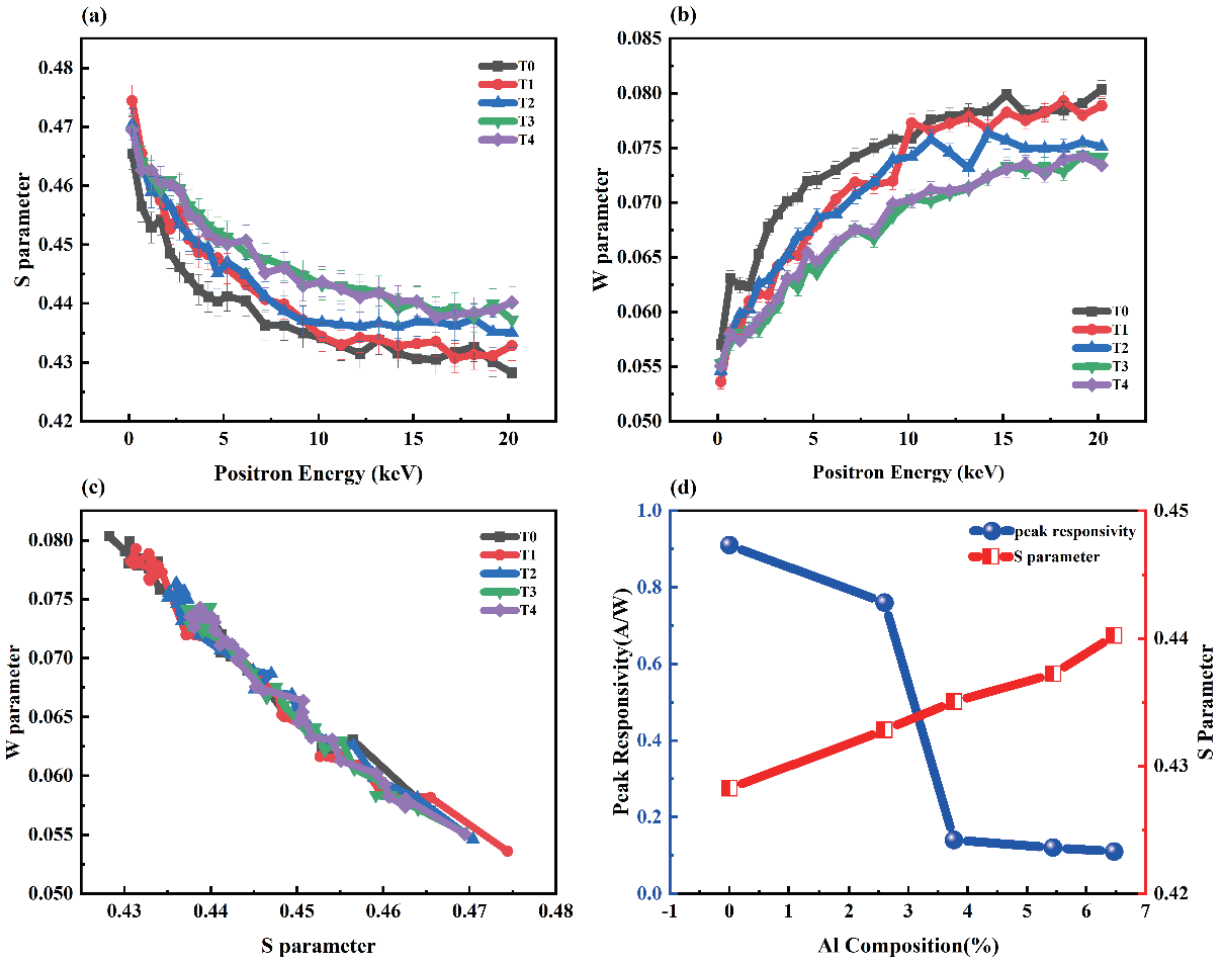

Fig. 4. (Color online) Dependence of the low momentum parameter *S* (a) and high momentum parameter *W* (b) on positron incident energy in these five samples. (c) Relationship between *S* and *W* of the five samples. (d) *S* parameter and peak responsivity of AlGaN detector versus AlN mole fraction of AlGaN.

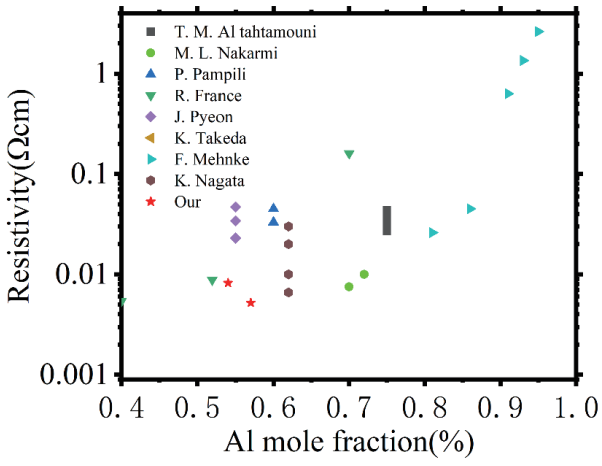

Fig. 5. (Color online) Previously reported resistivity value as a function of the AlN mole fraction of n-AlGaN layers. Our results are shown as red solid star symbols[33].

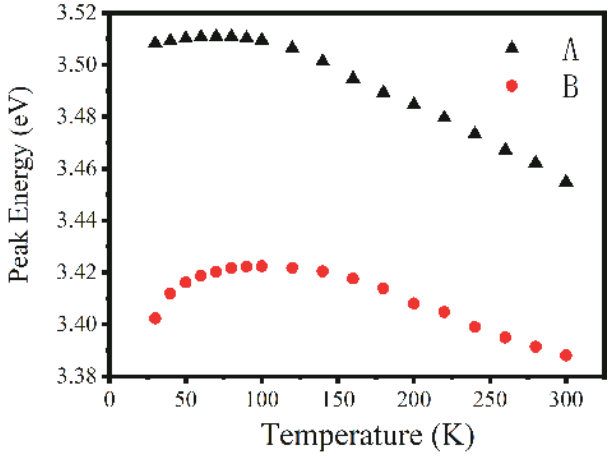

Fig. 6. (Color online) PL peak energy each as a function of temperature for samples A (3 nm) and B (6 nm).

UVA LDs usually are AlGaN, GaN, or InGaN with low InN mole fraction.

To increase the emission intensity of the UV quantum well, the emission mechanisms of GaN/AlGaN quantum well were studied by using temperature dependent photoluminescence (TDPL) and a 325 nm He–Cd continuous wave laser excitation. Two single GaN/AlGaN quantum well structures with different thicknesses of GaN quantum well of 3 and 6 nm were grown on the AlGaN template obtained by the method introduced in Section 3.1. They are named sample A and sample B, respectively. In these two samples, no other GaN layer is contained except for the GaN quantum well. Thus, the emission peak at about 360 nm comes from the GaN quantum well. The variations of peak energy with temperature are shown in Fig. 6. It is found that "V-shape" temperature dependence of

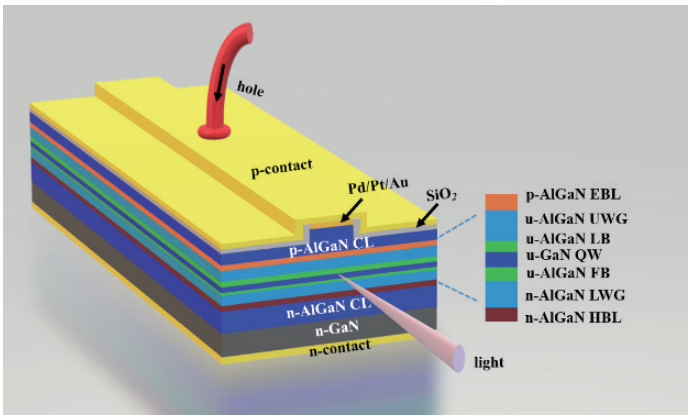

Fig. 7. (Color online) The schematic diagram of LD structure.

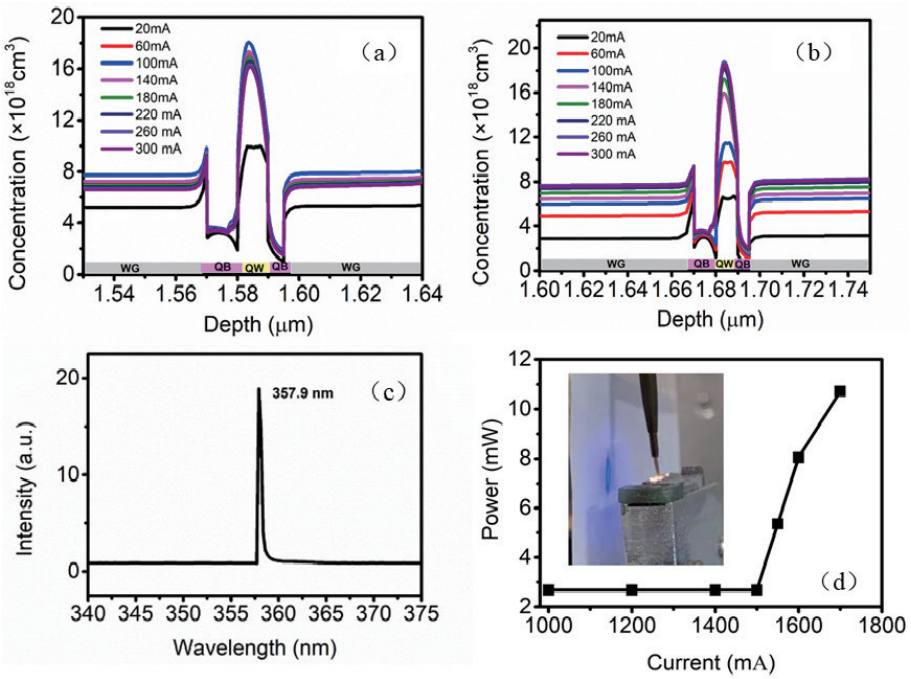

Fig. 8. (Color online) Spatial distribution of electron concentration around WG layers and active region under different injection current values from 20 to 300 mA for samples LD1 with 50 nm-thick WG layer (a), LD2 with 150 nm-thick WG layer (b). (c) Shows lasing wavelength of 357.9 nm in the electroluminescence spectrum of another UV LD under RT pulsed operation condition at an injection current of 1550 mA. (d) Shows the RT output power of the 357.9 nm LD as a function of injected current. The inset shows a photo of the laser with the blue far field pattern of the laser beam image formed on the white paper screen.

photoluminescence (PL) peak energy exists in these two samples, which is similar to the phenomenon observed in InGaN multiple quantum wells[22, 23]. This indicates that localized states also exist in GaN quantum wells. In addition, we found that the blueshift of the peak increases with increasing thickness of GaN quantum well, which suggests that the localization effect is enhanced for a thicker GaN quantum well. It also results in a longer emission wavelength of thicker GaN quantum well at room temperature. We speculated that localized states are induced by the fluctuations of layer thickness of GaN QWs. Thus, the introduction of modified localization effect in GaN QWs may be a method to enhance the emission efficiency of GaN/AlGaN QW active region.

3.4. Suppression of the leakage of carrier by designing the structure of UV LDs

For UV LDs with a lasing wavelength less than 370 nm, the optimized Al mole fraction of AlGaN cladding layers should be higher than 20%[1–6, 14–16] to obtain good optical confinement. However, this is too high to grow on free standing GaN substrate directly due to the huge stress between AlGaN cladding layers and GaN substrate. Two methods to grow a high AlN mole fraction AlGaN template layer were introduced in Section 3.1. However, the crystal quality of AlGaN cladding layers is not as good as that of AlGaN with lower AlN mole fraction when grown on GaN substrate. This will lead to an increase of threshold voltage and threshold current density of UV LDs[10, 27]. In order to achieve short lasing wavelength of UV LDs, on the one hand, we need to optimize the growth condition to improve crystalline quality of AlGaN cladding layer; while on the other hand, we can design the structure of UV LDs based on high quality low AlN mole fraction of AlGaN cladding layers.

A schematic diagram of LD structure is shown in Fig. 7, where the Al content of AlGaN CL is about 7% and the Al content of AlGaN waveguide (WG) layer is about 3%. The optical

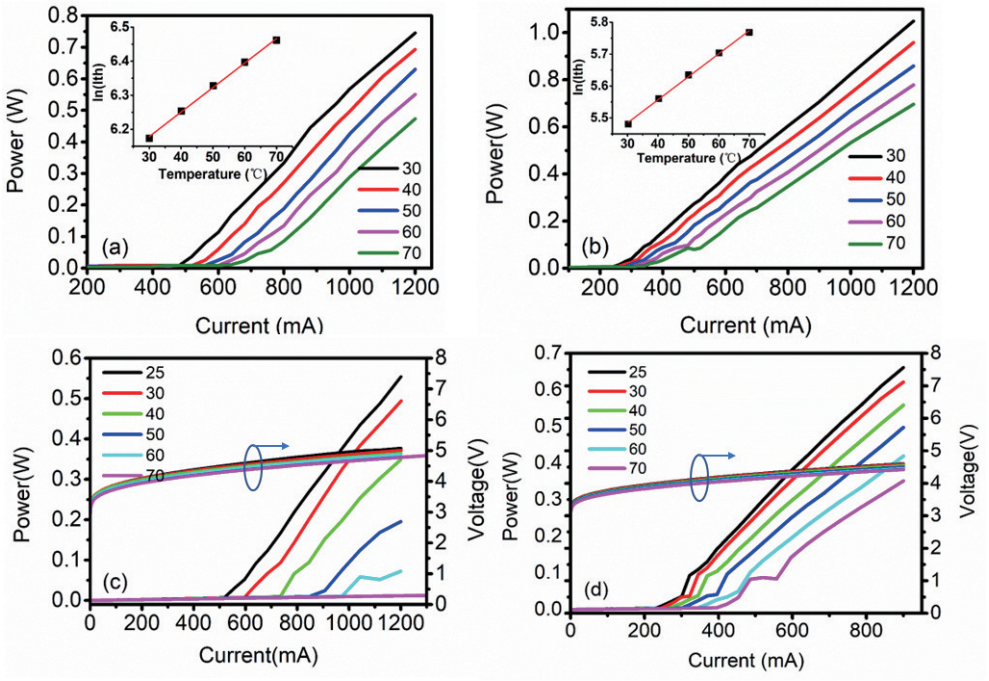

Fig. 9. (Color online) Pulsed light output power versus injection current of LD A (a) and LD B (b) as a function of temperature. Temperature dependences of CW *P*–*I*–*V* characteristics of LD A (c) and LD B (d). The insets of (a) and (b) show ln(I_{th}) as a function of temperature for LD A (a) and LD B (b).

confinement factor is higher than 4%[15], which is large enough for UV LDs[34, 35]. However, in this case, due to the small potential barrier energy between QW region, WG layers, and CL layers, the confinement effect for carriers is relatively weak, the carrier concentration in AlGaN upper WG layer will be relatively large, and more carriers stay and recombine in the UWG layer, as shown in Fig. 8. This leads to a reduction of the accumulation rate of carriers in QW region. The carriers in WG layers do not contribute to stimulated emission. Thus, a higher threshold current should result. In order to suppress the carrier loss in UWG layers, thinner AlGaN WG layers and an n-AlGaN hole block layer were used in UV LDs. A comparison of LD1 of Fig. 8(a) with LD2 of Fig. 8(b) shows that the accumulation rate of injected carriers in QW layer of LD1 increases and 366 nm UVA LD lasing was achieved[15]. Based on this modified structure, another UVA LD with lasing wavelength of 357.9 nm was also fabricated by using an increased AlN mole fraction of AlGaN WG layer[16]. The electroluminescence spectrum of the latter UV LD under room temperature (RT) pulsed operation condition at an injection current of 1550 mA is shown in Fig. 8(c), and its output power as a function of injected current measured at RT is shown in Fig. 8(d). The inset is a photo of the laser beam image formed on the white paper screen.

3.5. Suppression of thermal effect in UV LDs

UV LDs are potential light sources of various applications, such as ultraviolet curing and materials processing. For these applications, high output power is required to obtain, for example, high UV curing speed and quick cuttings of thick metal. In addition to the slope efficiency (SE) and threshold current of LDs, thermal rollover phenomenon at high injection current and the catastrophic optical mirror degradation (COMD) at facets are also limiting factors for their output power[1, 16]. Therefore, improving the characteristic temperature T_0 and reducing the junction temperature of UV LDs may be solutions for high power LDs. The thermal properties of GaN UV LDs have been reported by some research groups, Taketomi[12] and Crawford[28] *et al*. measured characteristic temperature T_0 of their UV LDs, it is 119 and 140 K in the temperature range of 20–60 °C, respectively. Tsuzuki *et al*.[27] fabricated a 358 nm UV LD with a high characteristic temperature T_0 of 174 K in the temperature range of 7–27 °C, they attribute higher T_0 to low density of dislocation or nonradiative recombination centers. Yoshida *et al*.[36] of Hamamatsu Corporation investigated the temperature characteristic of a GaN/AlGaN MQW LD with lasing wavelength of about 360 nm in detail. They have found that the characteristic temperature in the low temperature range is 130 K. Meanwhile, in the high temperature range, it drops down to a value of 90 K. They believe that the decrease of T_0 may be due to the increase of nonradiative recombination, as well as the increase of electron current overflow from the active region to the p-cladding layer at higher temperature.

We also study the thermal characteristics of two UV LDs with different WG structures LD A and LD B under pulsed and CW operation[17], as shown in Fig. 9. The lasing wavelength is 384 nm under CW operation. The WG layer thickness of LD B (120 nm) is larger than LD A (80 nm), the absorption loss of LD A is larger than that of LD B. The threshold current (I_{th}) increases and slope efficiency (SE) slightly decreases when the temperature increases from 30 to 70 °C. The relationship of ln(I_{th}) with the temperature (T) has been derived and is fitted by using linear relation for both LDs, as shown in the insets of Figs. 9 (a) and 9(b). The calculated characteristic temperature T_0 of LD A and LD B is 139 and 138 K, respectively. These values are comparable to those of previously reported UV-LDs in the literature[12, 27, 28, 36], and the temperature stability of LD B is close to that of LD A. However, under CW operation, the dependence of output power on temperature is

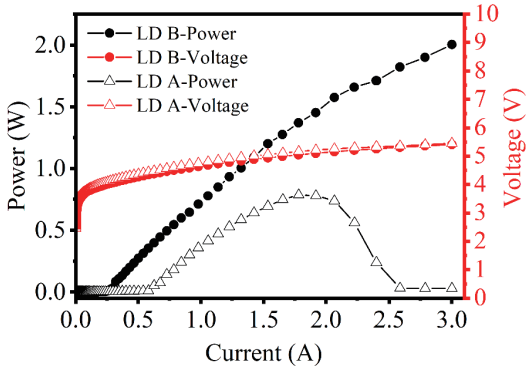

Fig. 10. (Color online) *P–I* and *I–V* curves of LD A (empty symbols) and LD B (full symbols) under CW operation for LD A and LD B.

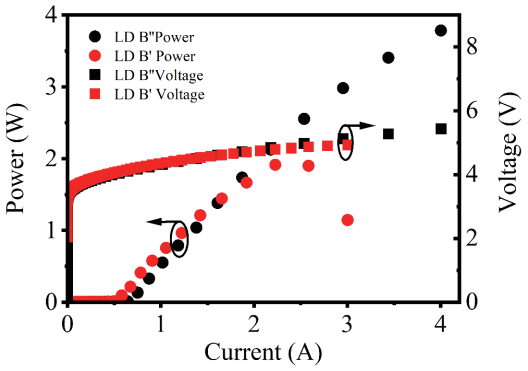

Fig. 11. (Color online) *I–V* curves (square points) and *P–I* curves (circle points) of LD B′ (red) and LD B″(black) under CW operation.

very different for LD A and LD B. For LD A, its I_{th} increases and SE decreases quickly with increasing temperature, and it does not lase, even though the injection current increases to 1.4 A at temperature of 70 °C. For LD B, the I_{th} increases and SE decreases much slower than those of LD A, and I_{th} increases only 150 mA when the measured temperature increases from 25 to 70 °C. The output power of LD A deteriorates larger than that of LD B with increasing temperature. This indicates that the junction temperature of LD A is higher than LD B under CW operation. This is attributed to the stronger self-heating effect of LD A due to larger optical absorption loss. Controlling junction temperature is more important for UV LDs operated under CW mode because they usually have lower characteristic temperature (T_0) compared with GaN based blue and violet LDs. Fig. 10 shows *P–I–V* curves of LD A and LD B measured from zero current to a large injection current of 3 A. The *I–V* curves of two LDs are quite similar to each other. However, the output power decreases when the injection current increases to higher than 1.9 A for LD A due to thermal rollover phenomenon, and such a phenomenon is not observed for LD B until 3 A. This indicates that the suppression of the self-heating effect to decrease the junction temperature is very important for high power CW UV LDs.

Another method to decrease the junction temperature is to use flip chip package (p-side down on sub-mount) to accelerate heat dissipation[18]. The chips were packaged with n-side down on sub-mount (named LD B′) or p-side down on sub-mount (named LD B″), respectively. Fig. 11 shows *I–V* and *P–I* curves of LDs under CW operation. The red date points are the output power and voltage date of LD B′ and the black points are the ones of LD B″. It can be seen that the output power increases with increasing injection current for both LD B′ and LD B″ at first, then it decreases when the injection current increases to higher than 2.4 A for LD B′ due to thermal rollover phenomenon, and such a phenomenon is not observed for LD B″ until 4 A. This indicates that the flip chip package (p-side down on sub-mount) is an effective method to accelerate heat dissipation and increase the maximum output power of UV LDs.

3.6. Mechanisms of cavity facet degradation for GaN-based laser diodes

Degradation mechanisms are a key factor to improve the reliability of GaN-based LDs. Many researchers have studied the degradation mechanisms of GaN based LDs previously.

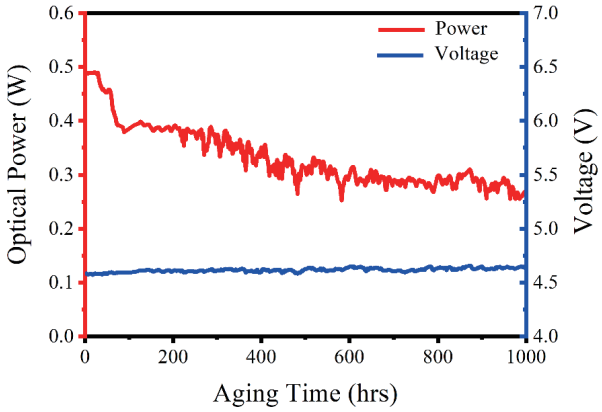

Fig. 12. (Color online) Optical output power curve (red) and the corresponding voltage curve (blue) as a function of the aging time for the unsealed LD under a CW operation with an injection current of 800 mA.

Some groups found that the degradation of active region is one reason for the degradation of GaN LDs[37–39], which can be attributed to the increase in nonradiative recombination due to the deep-level states induced by vacancy defects. Another reason is the variation of junction temperature, which is caused by the increase of the series resistance because of the degradation of the Ohmic contact. A higher junction temperature also leads to an increased leakage current[40] and a high non-radiative recombination rate. Catastrophic optical mirror damage (COMD) related to high power optical densities is also a common degradation mode occurring on the facet of LDs. The COMD in GaN-based LDs shows a thermal procedure for material decomposition, melting of (Al, In) GaN, and even a partial vaporization in active region and waveguide layers. A typical effect of the consequences of COMD in GaN-based LDs is the void cavities or gallium droplets on the facets[41–43].

One new mode of facet degradation was found during our experiment with unsealed blue-violet LDs with lasing wavelength of 434 nm[44]. The aging curve of the optical power and the corresponding voltage curve for the unsealed LD is shown in Fig. 12. The optical output power of the unsealed LD remains at a constant value within the initial 30 h and then decreases accompanied by an irregular undulation of the output power. The voltage remained unchanged during the testing process. This indicates that neither deterioration of the electrode quality nor leakage currents occurs during

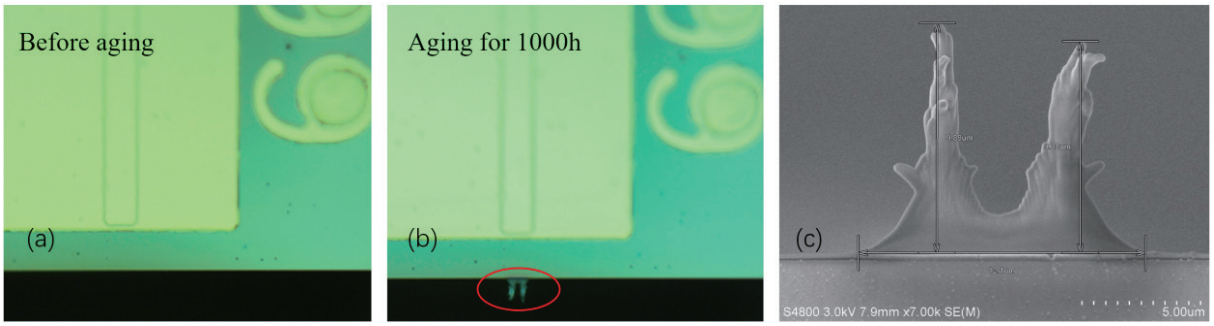

Fig. 13. (Color online) Optical micrographs of the top view of LD front cavity facet for virgin (a) and aged (b) LD, respectively, where the waveguide ridge region can be seen by two green parallel lines. The deposits at front facet are marked by a red ellipsoidal circle in (b). SEM images (c) of the front cavity facet for aged LD. A biforked deposit is clearly observed in the side view.

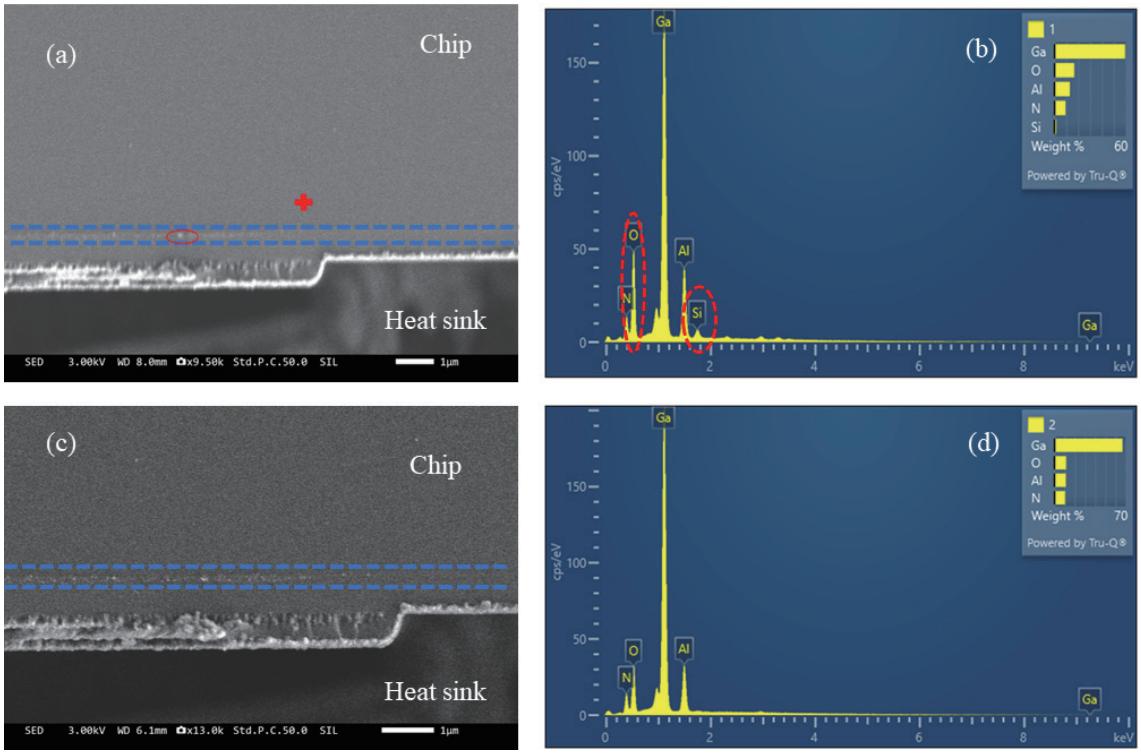

Fig. 14. (Color online) (a) SEM images of the front cavity facet for aged flip chip packaged LD with lasing wavelength of 384 nm, where the QW region is located between two parallel dashed blue lines; (c) is the enlarged image of (a) under ridge region; (b) and (d) are the EDS images for the regions in (a) marked with red ellipsoidal circle and thick red crosshair, respectively.

testing. Fig. 13 presents the images of the front facet for the initial and aged LDs. A biforked deposit was observed on the facet after 1000 h of aging. Deposit growth is believed to be responsible for the undulation of the optical power during the degradation of the unsealed LD. With an increase in the sediment thickness, the reflectance of the facet changes, and thus the resonance property of the cavity is partially damaged. Energy dispersive X-ray spectrometer (EDS) mapping was employed to analyze the chemical composition of the sediment. This reveals that the sediment is composed of the elements of silicon (Si), oxygen (O), aluminum (Al), and gallium (Ga) with different atomic percentages, respectively. According to the analysis, Al and Ga elements are from Al_2O_3 front facet coating and GaN epilayer. The biforked deposit should be SiO_2. It is proposed that the splitting of water molecules induced by high-energy photons triggers the deposition of SiO_2[44]. The deposits on the facet should be responsible for the reduction of the LDs' output power.

For UV LDs with higher energy of photons, the facet degradation should be more serious. White spot deposits were observed only in the front cavity facet around MQW region below ridge in UV LDs after 48 h of aging and is not observed outside the ridge, as shown in Figs. 14(a) and 14(c), where MQW region is between two blue dotted line. This indicates that the formation of the white spot deposits in cavity is related to laser action. Figs. 14(b) and 14(d) are the EDS images for the regions in Fig. 14(a) marked with red ellipsoidal circle and thick red crosshair, respectively. It is found that the location of white spot deposits contains higher concentration of Si and O elements. There should be SiO_2. The mechanism should be similar to the facet degradation mechanism observed in the blue-violet LDs[44] but the GR of deposits is much faster. Thus, improving the tightness of device package is necessary to avoid the fast degradation of GaN-based LDs, especially for UV LDs. In addition, an increase of nonradiative recombination in active region was observed

in UV LDs. The related experimental data are being sorted out and will be published later.

4. Summary

In this paper, we outline major challenges in the realization of UV LDs and the technologies required to respond to them. In order to improve the performance of UV LDs, a thick layer of high crystal quality AlGaN film without cracking, a high emission efficiency active region, a good optical waveguide structure, and a relatively low junction working temperature are important. In order to relieve the mismatch stress of the AlGaN template, we used a AlN modulation layer to change the growth mode of AlGaN layer, a high crystal quality AlGaN film without cracking was obtained. The emission mechanism, cavity facet degradation mechanisms, and the optimized design of device structure for UV LDs were studied. With these techniques, RT pulsed oscillation of AlGaN UVA LD has been realized, whose lasing wavelength is 357.9 nm. Combined with the suppression of thermal effect, the high output power of 3.8 W UV LD with lasing wavelength of 386.5 nm was also fabricated.

Acknowledgment

This work was supported by the National Key R&D Program of China (2022YFB3605104); National Natural Science Foundation of China (62250038, 61904172, 61974162, 62034008, 62074142, and 62074140); Strategic Priority Research Program of Chinese Academy of Sciences (XDB43030101); Shanxi-Zheda Institute of Advanced Materials and Chemical Engineering (2022SX-TD016).

References

[1] Nagata K, Takeda K, Nonaka K, et al. Reduction in threshold current density of 355 nm UV laser diodes. Phys Status Solidi C, 2011, 8, 1564

[2] Iida K, Kawashima T, Miyazaki A, et al. Laser diode of 350.9 nm wavelength grown on sapphire substrate by MOVPE. J Cryst Growth, 2004, 272, 270

[3] Yamashita Y, Kuwabara M, Torii K, et al. A 340-nm-band ultraviolet laser diode composed of GaN well layers. Opt Express, 2013, 21, 3133

[4] Aoki Y, Kuwabara M, Yamashita Y, et al. A 350-nm-band GaN/AlGaN multiple-quantum-well laser diode on bulk GaN. Appl Phys Lett, 2015, 107, 151103

[5] Nagahama S I, Yanamoto T, Sano M, et al. Study of GaN-based laser diodes in near ultraviolet region. Jpn J Appl Phys, 2002, 41, 5

[6] Masui S, Matsuyama Y, Yanamoto T, et al. 365 nm ultraviolet laser diodes composed of quaternary AlInGaN alloy. Jpn J Appl Phys, 2003, 42, L1318

[7] Zhang Z Y, Kushimoto M, Sakai T, et al. A 271.8 nm deep-ultraviolet laser diode for room temperature operation. Appl Phys Express, 2019, 12, 124003

[8] Niass M I, Sharif M N, Wang Y F, et al. A contrivance of 277 nm DUV LD with $B_{0.313}Ga_{0.687}N/B_{0.40}Ga_{0.60}N$ QWs and $Al_xGa_{1-x}N$ heterojunction grown on AlN substrate. J Semicond, 2019, 40, 122802

[9] Nakamura S, Senoh M, Nagahama S I, et al. InGaN/GaN/AlGaN-based laser diodes with modulation-doped strained-layer superlattices grown on an epitaxially laterally overgrown GaN substrate. Appl Phys Lett, 1998, 72, 211

[10] Yoshida H, Yamashita Y, Kuwabara M, et al. A 342-nm ultraviolet AlGaN multiple-quantum-well laser diode. Nature Photon, 2008, 2, 551

[11] Yoshida H, Yamashita Y, Kuwabara M, et al. Demonstration of an ultraviolet 336 nm AlGaN multiple-quantum-well laser diode. Appl Phys Lett, 2008, 93, 241106

[12] Taketomi H, Aoki Y, Takagi Y, et al. Over 1 W record-peak-power operation of a 338 nm AlGaN multiple-quantum-well laser diode on a GaN substrate. Jpn J Appl Phys, 2016, 55, 05FJ05

[13] Zhang Z Y, Kushimoto M, Yoshikawa A, et al. Key temperature-dependent characteristics of AlGaN-based UV-C laser diode and demonstration of room-temperature continuous-wave lasing. Appl Phys Lett, 2022, 121, 222103

[14] Zhao D G, Yang J, Liu Z S, et al. Fabrication of room temperature continuous-wave operation GaN-based ultraviolet laser diodes. J Semicond, 2017, 38, 051001

[15] Yang J, Wang B B, Zhao D G, et al. Realization of 366 nm GaN/AlGaN single quantum well ultraviolet laser diodes with a reduction of carrier loss in the waveguide layers. J Appl Phys, 2021, 130, 173105

[16] Yang J, Zhao D G, Liu Z S, et al. A 357.9 nm GaN/AlGaN multiple quantum well ultraviolet laser diode. J Semicond, 2022, 43, 010501

[17] Yang J, Zhao D G, Liu Z S, et al. Room temperature continuous-wave operated 2.0-W GaN-based ultraviolet laser diodes. Opt Lett, 2022, 47, 1666

[18] Yang J, Zhao D G, Liu Z S, et al. Regulating absorption loss and carrier injection efficiency in ultraviolet laser diodes by changing waveguide layer structure. Opt Laser Technol, 2022, 156, 108574

[19] Amano H, Collazo R, De Santi C, et al. The 2020 UV emitter roadmap. J Phys D: Appl Phys, 2020, 53, 503001

[20] Guenther B D, Steel D G. Encyclopedia of modern optics. Academic Press, 2018

[21] Guo Q A, Kirste R, Mita S, et al. Design of AlGaN-based quantum structures for low threshold UVC lasers. J Appl Phys, 2019, 126, 223101

[22] Cho Y H, Gainer G H, Fischer A J, et al. "S-shaped" temperature-dependent emission shift and carrier dynamics in InGaN/GaN multiple quantum wells. Appl Phys Lett, 1998, 73, 1370

[23] Yang J, Zhao D G, Jiang D S, et al. Optical and structural characteristics of high indium content InGaN/GaN multi-quantum wells with varying GaN cap layer thickness. J Appl Phys, 2015, 117, 055709

[24] Yoshida H, Takagi Y, Kuwabara M, et al. Entirely crack-free ultraviolet GaN/AlGaN laser diodes grown on 2-in. sapphire substrate. Jpn J Appl Phys, 2007, 46, 5782

[25] Wang B B, Yang J, Zhao D G, et al. The mechanisms of AlGaN device buffer layer growth and crystalline quality improvement: Restraint of gallium residues, mismatch stress relief, and control of aluminum atom migration length. Crystals, 2022, 12, 1131

[26] Ji Q B, Li L, Zhang W, et al. Dislocation reduction and stress relaxation of GaN and InGaN multiple quantum wells with improved performance via serpentine channel patterned mask. ACS Appl Mater Interfaces, 2016, 8, 21480

[27] Tsuzuki H, Mori F, Takeda K, et al. High-performance UV emitter grown on high-crystalline-quality AlGaN underlying layer. Phys Status Solidi (a), 2009, 206, 1199

[28] Crawford M H, Allerman A A, Armstrong A M, et al. Laser diodes with 353 nm wavelength enabled by reduced-dislocation-density AlGaN templates. Appl Phys Express, 2015, 8, 112702

[29] Zhao D G, Jiang D S, Yang H, et al. Effect of lightly Si doping on the minority carrier diffusion length in n-type GaN films. Appl Phys Lett, 2006, 88, 252101

[30] Warnick K H, Puzyrev Y, Roy T, et al. Room-temperature diffusive phenomena in semiconductors: The case of AlGaN. Phys Rev B, 2011, 84, 214109

[31] Puzyrev Y S, Roy T, Beck M, et al. Dehydrogenation of defects and

hot-electron degradation in GaN high-electron-mobility transistors. J Appl Phys, 2011, 109, 034501
[32] Huang Y J, Yang J, Zhao D G, et al. Role of vacancy defects in reducing the responsivity of AlGaN Schottky barrier ultraviolet detectors. Nanomaterials, 2022, 12, 3148
[33] Yang J, Zhang Y H, Zhao D G, et al. Realization low resistivity of high AlN mole fraction Si-doped AlGaN by suppressing the formation native vacancies. J Cryst Growth, 2021, 570, 126245
[34] Zhang L Q, Jiang D S, Zhu J J, et al. Confinement factor and absorption loss of AlInGaN based laser diodes emitting from ultraviolet to green. J Appl Phys, 2009, 105, 023104
[35] Chen P, Feng M X, Jiang D S, et al. Improvement of characteristics of InGaN-based laser diodes with undoped InGaN upper waveguide layer. J Appl Phys, 2012, 112, 113105
[36] Yoshida H, Kuwabara M, Yamashita Y, et al. The Current status of ultraviolet laser diodes. Phys Status Solidi A, 2011, 208, 1586
[37] Marona L, Wisniewski P, Prystawko P, et al. Degradation mechanisms in InGaN laser diodes grown on bulk GaN crystals. Appl Phys Lett, 2006, 88, 201111
[38] Takeya M, Mizuno T, Sasaki T, et al. Degradation in AlGaInN lasers. Phys Stat Sol (c), 2003, 7, 2292
[39] Meneghini M, Carraro S, Meneghesso G, et al. Degradation of InGaN/GaN laser diodes investigated by micro-cathodoluminescence and micro-photoluminescence. Appl Phys Lett, 2013, 103, 233506
[40] Marona L, Wiśniewski P, Leszczyński M, et al. Why InGaN laser-diode degradation is accompanied by the improvement of its thermal stability. Integrated Optoelectronic Devices 2008, 2008, 68940R
[41] Mura G, Vanzi M, Hempel M, et al. Analysis of GaN based high-power diode lasers after singular degradation events. Physica Rapid Research Ltrs, 2017, 11, 1700132
[42] Tomm J W, Kernke R, L Löffler, et al. Defect evolution during catastrophic optical damage in 450-nm emitting InGaN/GaN diode lasers. SPIE 10553, Novel in-Plane Semiconductor Lasers XVII, 2018, 1055308
[43] Strauss U, Somers A, Heine U, et al. GaInN laser diodes from 440 to 530nm: a performance study on single-mode and multi-mode R&D designs. Proc SPIE 10123, Novel in-Plane Semiconductor Lasers XVI, 2017, 101230A
[44] Wang X W, Liu Z S, Zhao D G, et al. New mechanisms of cavity facet degradation for GaN-based laser diodes. J Appl Phys, 2021, 129, 223106

Jing Yang received her Ph.D. from the University of Chinese Academy of Sciences (UCAS) in 2015. She then joined the Institute of Semiconductors, Chinese Academy of Sciences. She is currently an associate research fellow. Her current research interests include metal organic chemical vapor deposition growth of III-Nitride material and devices, especially in GaN-based ultra violet and green laser diodes. She joined in the Youth Innovation Promotion Association of Chinese Academy of Sciences in 2019, and won the Beijing Nova Program in 2020.

Degang Zhao received his B.Sc. and M.Sc. degrees from the University of Electronic Science and Technology of China in 1994 and 1997, respectively. He received his Ph.D. from the Chinese Academy of Sciences in 2000. Later on, he joined in Institute of Semiconductors, Chinese Academy of Sciences, Beijing. He won the National Natural Science Foundation for Distinguished Young Scholars in 2009, and won the National Award for Youth in Science and Technology of China in 2011. His research interests are mainly focused on GaN-based optoelectronic materials and devices, such as laser diodes and ultraviolet photodetectors. He has many research achievements in material growth and device fabrication, and has authored or co-authored over 300 articles in refereed journals and holds more than 40 patents.